AD-A190 132 ANALYSIS OF DUCTILE-BRITTLE TRANSITION TEMPERATURES FOR CONTROLLED-ROLLED.. (U) DAVID TAYLOR RESEARCH CENTER BETHESDA MD SHIP MATERIALS ENGIN.. 1/1

UNCLASSIFIED R W ARMSTRONG ET AL. MAY 88 DTRC/SME-88-30 F/G 11/6.1 NL

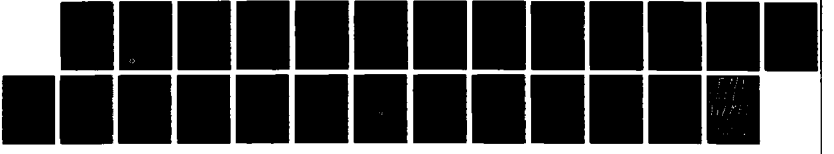

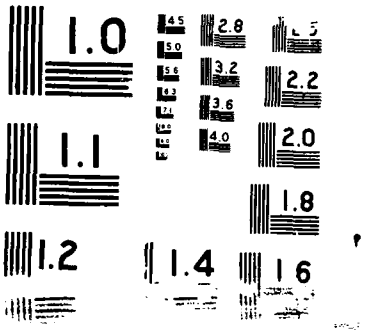
1.0
1.1
1.2
1.4
1.6
1.8
2.0
2.2
2.8
3.2
3.6
4.0
4.5
5.0
5.6

(4)

David Taylor Research Center

Bethesda, Maryland 20084-5000

DTRC/SME-88-30 May 1988

Ship Materials Engineering Department

Research and Development Report

ANALYSIS OF DUCTILE-BRITTLE TRANSITION TEMPERATURES FOR CONTROLLED-ROLLED, MICROALLOYED, C-Mn BASED STEELS

by

R. W. Armstrong

L. R. Link

G. R. Speich

DTRC/SME-88-30 Analysis of Ductile-Brittle Transition Temperatures for Controlled-Rolled, Microalloyed, C-Mn Based Steels

UNCLASSIFIED

SECURITY CLASSIFICATION OF THIS PAGE

REPORT DOCUMENTATION PAGE

1a REPORT SECURITY CLASSIFICATION UNCLASSIFIED	1b RESTRICTIVE MARKINGS
2a SECURITY CLASSIFICATION AUTHORITY	3 DISTRIBUTION / AVAILABILITY OF REPORT Approved for public release; distribution unlimited.
2b DECLASSIFICATION / DOWNGRADING SCHEDULE	
4 PERFORMING ORGANIZATION REPORT NUMBER(S) DTRC/SME-88-30	5 MONITORING ORGANIZATION REPORT NUMBER(S)
6a NAME OF PERFORMING ORGANIZATION David Taylor Research Center 6b OFFICE SYMBOL (If applicable) 2814	7a NAME OF MONITORING ORGANIZATION
6c ADDRESS (City, State, and ZIP Code) Bethesda, MD 20084-5000	7b ADDRESS (City, State, and ZIP Code)
8a NAME OF FUNDING / SPONSORING ORGANIZATION DTRC 8b OFFICE SYMBOL (If applicable) 0115	9 PROCUREMENT INSTRUMENT IDENTIFICATION NUMBER
8c ADDRESS (City, State, and ZIP Code) Bethesda, MD 20084-5000	10 SOURCE OF FUNDING NUMBERS PROGRAM ELEMENT NO: 62234N; PROJECT NO:; TASK NO.: RS34S50; WORK UNIT ACCESSION NO.: DN507603

11 TITLE (Include Security Classification)
ANALYSIS OF DUCTILE-BRITTLE TRANSITION TEMPERATURES FOR CONTROLLED-ROLLED, MICROALLOYED, C-Mn BASED STEELS

12 PERSONAL AUTHOR(S)
R.W. Armstrong, L.R. Link, G.R. Speich

13a TYPE OF REPORT	13b TIME COVERED	14 DATE OF REPORT (Year, Month, Day)	15 PAGE COUNT
R&D	FROM 12/86 TO 12/87	May 1988	25

16 SUPPLEMENTARY NOTATION
1-2803-117-20

17 COSATI CODES			18 SUBJECT TERMS (Continue on reverse if necessary and identify by block number)
FIELD	GROUP	SUB-GROUP	Ductile-brittle transition temperature, C-Mn steel, carbide plate effects. (SRS)

19 ABSTRACT (Continue on reverse if necessary and identify by block number)

Charpy V-notch ductile-brittle transition temperatures reported for a conventional ~~C-Mn~~ Carbon Manganese steel and for several controlled-rolled microalloyed steels are compared with transition temperatures computed on a dislocation model basis. The computed transition temperature, T_c, is specified by equating the tensile cleavage fracture stress and the effective yield stress at the Charpy V-notch. Increased friction stress resistances to dislocation movement provided by solutes, precipitates, and other dislocations raise the yield stress and, thereby, increase T_c. A residual dislocation based friction stress resistance occurs within untransformed ferrite grains (that is, the ferrite present at the rolling temperature) when finish rolling is done in the austenite-ferrite region. Grain size refinement normally lowers T_c because the cleavage stress is increased to a greater extent than is the yield stress. When cleavage is controlled by the growth of a crack from grain boundary carbide, as might occur in a low-carbon microalloyed steel, T_c is raised to an increased extent as the ratio of ferrite grain diameter and carbide plate thickness is smaller.

20 DISTRIBUTION / AVAILABILITY OF ABSTRACT	21 ABSTRACT SECURITY CLASSIFICATION	
☒ UNCLASSIFIED/UNLIMITED ☐ SAME AS RPT ☐ DTIC USERS		
22a NAME OF RESPONSIBLE INDIVIDUAL L.R. Link	22b TELEPHONE (Include Area Code) (301) 267-4335	22c OFFICE SYMBOL DTRC 2814

DD FORM 1473, 84 MAR 83 APR edition may be used until exhausted
All other editions are obsolete

SECURITY CLASSIFICATION OF THIS PAGE

UNCLASSIFIED

CONTENTS

FIGURES

TABLES

ABBREVIATIONS

α	Triaxial stress state at a notch
$\dot{\epsilon}$	Strain rate
FATT	Fracture appearance transition temperature
G	Shear modulus
k_y	Microstructural stress intensity
ℓ	Grain diameter
σ_c	Cleavage fracture stress
σ_G	Athermal stress component of the friction stress
σ_o	Friction stress
σ_{TH}	Thermal stress component of the friction stress
σ_y	Yield stress
TASRA	Thermal activation-strain rate analysis
T_c	Transition temperature
t	Carbide plate thickness
γ_p	Surface energy
ν	Poisson's ratio

ABSTRACT

Charpy V-notch ductile-brittle transition temperatures reported for a conventional C-Mn steel and for several controlled-rolled microalloyed steels are compared with transition temperatures computed on a dislocation model basis. The computed transition temperature, T_c, is specified by equating the tensile cleavage fracture stress and the effective yield stress at the Charpy V-notch. Increased friction stress resistances to dislocation movement provided by solutes, precipitates, and other dislocations raise the yield stress and, thereby, increase T_c. A residual dislocation based friction stress resistance occurs within untransformed ferrite grains (that is, the ferrite present at the rolling temperature) when finish rolling is done in the austenite-ferrite region. Grain size refinement normally lowers T_c because the cleavage stress is increased to a greater extent than is the yield stress. When cleavage is controlled by the growth of a crack from grain boundary carbide, as might occur in a low-carbon microalloyed steel, T_c is raised to an increased extent as the ratio of ferrite grain diameter and carbide plate thickness is smaller.

ADMINISTRATIVE INFORMATION

This report was prepared as part of the Materials and Fabrication Block Program under the sponsorship of Mr. Ivan Caplan, David Taylor Research Center (DTRC Code 011.5). The effort was supervised by Mr. T. W, Montemarano, DTRC Code 2814, under Program Element Number 62234N, Task Area RS 34S50, Work Unit 1-2814-208. This report satisfies FY87 Milestone 2803-117 .

CONTROLLED-ROLLED STEEL PROPERTIES

Speich and Dabkowski (1) have reported ferrite grain diameter, ℓ, yield strength, σ_y, and fracture appearance transition temperature, FATT, measurements obtained for controlled-rolled C, C-Mn, C-Mn-Nb, and C-Mn-Mo-Nb steels. The steels were finish-rolled in the austenite or austenite-ferrite regions of the phase diagram. Substantially different finishing temperatures were involved. Inclusive of all the steels, a wide range in resultant ℓ values was obtained.

Figure 1 shows the influence of finishing temperature on the yield stress-grain size dependence for each steel. The experimental results are plotted on a Hall-Petch basis (2,3) as

$$\sigma_y = \sigma_o + k_y \ell^{-\frac{1}{2}} \qquad (1)$$

where different friction stress, σ_o, resistances are shown for the different steels as compared with their having the same slope, k_y, value, recently described as a microstructural stress intensity (4). The lower dashed reference line in Figure 1, following Equation (1), was shown previously by Morrison (5) to apply for low carbon steels over a wide range of grain diameters.

The trend established for the steels in Figure 1 is that the yield stress first increases at lowered austenitic finishing temperatures because of ferrite grain size refinement, whereas, at the lowest finishing temperatures in the austenite-ferrite region, σ_y increases because deformation of untransformed ferrite occurs during finishing. This deformation gives an increase in friction stress without much further reduction in grain size. Solid solution and precipitation strengthening are shown to have raised σ_o for the alloy steels even when finished at the highest temperatures.

An interesting comparison occurs in Figure 1 at the arrow markers for the C-Mn-Nb and C-Mn-Mo-Nb steels. Relatively greater ferrite grain size reduction was

proposed to occur for the latter steel at all finishing temperatures because of the measured effect of Mo on lowering the ferrite transformation temperature (1). The precipitation of NbC in the ferrite was consequently retarded, hence, a lower initial value of σ_o was measured relative to that for the C-Mn-Nb steel. Dilatometric measurements indicated that as much as 45% ferrite was present during controlled rolling of the C-Mn-Mo-Nb steel at 760°C. Yet, finishing at this temperature left σ_o unchanged. Very probably, Mo, through its solid solution strengthening of ferrite, particularly at 760°C in the austenite-ferrite region, caused the major portion of finishing deformation to be borne by the austenite. In this way the Mo addition to the alloy would have contributed very significantly to greater grain size reduction in the newly transformed ferrite, with a much lesser effect on σ_o overall because of the less heavily strained untransformed ferrite.

The influence of finishing temperature on the measured FATT-$\ell^{-\frac{1}{2}}$ relationship is shown in Figure 2. The dependence is especially interesting because of the reversal in behavior which occurs for the FATT. Beginning from relatively large grain diameters for each steel, that is, small $\ell^{-\frac{1}{2}}$ values, linear decreases in the FATT are shown with decrease in finishing temperature and increase in $\ell^{-\frac{1}{2}}$. The linear dependences of the different FATT values on $\ell^{-\frac{1}{2}}$ are in reasonable agreement with the dashed line (slope) dependence shown from previous transition temperature measurements reported for annealed steel materials by Heslop and Petch (6). The reversed behavior of an increase in FATT with increase in $\ell^{-\frac{1}{2}}$, observed beyond a minimum FATT value in each case, is seen by referring to Figure 1, to have occurred when the increase in σ_y was produced by an increase in σ_o. This is clearly established for the C-Mn steel results. The C-Mn-Mo-Nb steel results in Figure 2 show the beneficial effect on the FATT from a lower σ_o and continued reduction in grain size.

DISLOCATION MODEL ANALYSIS FOR T_c

Grain size and friction stress influences on the notch-sensitive ductile-brittle transition properties of materials can be obtained from the Hall-Petch dislocation pile-up based equations for σ_y and the cleavage fracture stress, σ_c. At transition the relationship between the stresses is as follows (7-9).

$$\sigma_c = \alpha\sigma_y(T,\varepsilon) \qquad (2)$$

where α is a measure of the triaxiality of the stress state at the notch; and, emphasis is given in the equation to the temperature, T, and strain rate, ε, dependences of σ_y. The Hall-Petch constants for σ_c have now been measured at relatively low T or high ε such that cleavage occurred before the condition of general plastic yielding was reached. The experimental constants, σ_{oc} and k_c, are essentially athermal and related to their σ_y counterparts by the inequalities : $\sigma_{oc} < \sigma_o$ and $k_c > k_y$. The latter inequality is supported by the dislocation theory prediction that a greater microstructural stress intensity is required to initiate cleavage than is required for general plastic yielding.

The thermal activation-strain rate analysis (TASRA) for plastic straining by dislocation movement within single crystals or polycrystal grains accounts for σ_o in terms of an athermal stress component, σ_G, and a thermal stress component, σ_{Th}, dependent also on ε. The stress components are combined in the equation

$$\sigma_o = \sigma_G + B_o\exp-\left[\beta_o - \beta_1\ln\varepsilon\right]T \qquad (3)$$

where B_o, β_o and β_1 are experimental constants evaluated in terms of dislocation model calculations (10). Experimentally, B_o is the value of σ_{Th} at T=0. The constants β_o and β_1 are determined from the strain rate dependence of the different bracketed slope values obtained from ln σ_{Th} plotted against T at various constant ε values. Table 1 gives comparable values of the TASRA constants determined in this

Table 1. Temperature, T, and strain rate, $\dot{\varepsilon}$, parameters (B_o,β_o,β_1) for the thermal component of friction stress (10): $\sigma_{Th}=B_o\exp-[\beta_o-\beta_1\ln\dot{\varepsilon}]T$, for mild steel (11), C-Mn steel (12), and Armco iron (13).

ℓ μm	σ_c MPa	T_{NDT} °K,meas.	$T_c\{\sigma_c\}$ °K	t μm	σ_c' MPa	$T_c\{\sigma_c'\}$ °K
10	1400	≈180	160	0.8	1296	185
20	1087	≈220	220	1.2	1028	240
65	750	≈280	317	2.0	724	331

way from measurements on related steel materials (11-13). Most measurements have indicated that k_y is athermal so that the total temperature and strain rate dependence of σ_y is in σ_o.

By substitution into Equation (2) of the Hall-Petch parameters for σ_c and of the terms for σ_o from Equation (3), with k_y included also, then, the ductile-brittle transition temperature, $T=T_c$, is obtained as

$$T_c = \left[\frac{1}{\beta_o - \beta_1 \ln\dot{\varepsilon}}\right]\left[\ln(\alpha B_o) - \ln\left[(k_c - \alpha k_y)\ell^{-\frac{1}{2}} + (\sigma_{oc} - \alpha\sigma_G)\right]\right] \qquad (4)$$

Equation (4) gives a quantitative guide for the explicit lowering of T_c by the several variables of grain size refinement, reduction in athermal friction stress, and for testing at a reduced strain rate (8,9). Sandstrom and Bergstrom (12) have employed the same type of analysis as given above, but they have neglected β_o in

Equation (3), to describe their measurements of the nil ductility Charpy V-notch transition temperature dependence on grain size for a C-1.32Mn mild steel. Their measurements have been employed in Equation (3) to obtain the B_o, β_o, and β_1 values given in Table 1.

Equation (4) has been applied in the present study, with further assistance from other measurements reported by Sandstrom and Bergstrom, to computing T_c for the 0.06C-1.26Mn steel results reported by Speich and Dabkowski (1). Sandstrom and Bergstrom computed tensile cleavage fracture stresses from notched bend test results obtained for various grain sizes and determined σ_{oc}=300 MPa and k_c=107 N/mm$^{3/2}$. They estimated that values of α=1.94 and ε=400s^{-1} were appropriate for the Charpy V-notch test measurements. With k_y=17.9 N/mm$^{3/2}$ for the C-Mn results in Figure 1 and a computed value of $\sigma_{Th}\approx$40 MPa at $\varepsilon\approx 3\times10^{-4}$ s^{-1}, then, $\sigma_G\approx$84 MPa for the fully austenitic finished material. The increases in σ_o shown at the smallest grain sizes in Figure 1 are attributed to added increases in σ_G. The values of T_c, thus computed from the total information put into Equation (4), are shown in Figure 3, superposed on the graph of FATT measurements reported by Speich and Dabkowski (1). With the exception of one point, at σ_y=300 MPa, remarkable agreement is obtained between the computed T_c and measured FATT values.

Detailed comparisons of the transition temperatures and their differences are listed in Table 2. By comparison of Figures 1-3, the initial decrease in T_c with increase in σ_y in Figure 3 has been attributed solely to a reduction in grain size, and the subsequent increase in T_c, attributed to an increase in σ_G. In fact, the computed lowering of T_c through grain size reduction, though greater than that indicated experimentally for the C-Mn steel, is in line with that indicated in Figure 3 for the grain size reduction effect on the FATT of all of the other steels. This is encouraging because an examination of Equation (4) shows that the

Table 2. Comparison of measured (1) and computed grain size and friction stress influences on ductile-brittle transition temperatures.

$\ell^{-\frac{1}{2}}$ $mm^{-\frac{1}{2}}$	σ_G MPa	FATT °C, meas.	T_C °C, calc.	FATT/$\Delta\ell^{-\frac{1}{2}}$ meas.	$T_C/\Delta\ell^{-\frac{1}{2}}$ calc.
6.5	84	-59	-59	-11	≈ -18
9.0	84	-87	-109		
				FATT/ σ_y meas.	$T_C/\ \sigma_G$ calc.
9.5	141	-81	-89	0.33	0.49
9.5	201	-59	-59		0.34

grain size dependence of T_c should be similar for the different steels. Figure 2 gives some experimental support for this consideration. The computed increase in T_c with increase in friction stress seems quite reasonable. Speich and Dabkowski attributed the increase in T_c to the occurrence of splitting failures. The indication is that the magnitude of the friction stress change associated with splitting is the major factor to consider when this type of behavior occurs.

THE INFLUENCE OF GRAIN BOUNDARY CARBIDE

A factor to consider for having contributed to the relatively high value of the FATT measurement at σ_y=300 MPa in Figure 3 is that cleavage fracture may have been promoted at this particular grain size because of the presence of carbide plates formed at some boundaries within the totally transformed ferrite grains. The situation has been analyzed recently by Petch (14). From his analysis, the lowered cleavage fracture stress, σ_c', for unstable growth of a cleavage crack from a grain boundary carbide plate of thickness, t, is obtained as

$$\sigma_c' = k_c t^{-1/2}\left[\left[1 - \frac{1}{8\pi^2}\frac{k_y^2}{k_c^2 t}\right]^{1/2} - \frac{1}{2\sqrt{2\pi}}\left[\frac{k_y}{k_c}\right]\left[\frac{\ell}{t}\right]^{1/2}\right] \qquad (5)$$

where k_c is specified as

$$k_c = \left[8G\gamma_p/\pi(1-\nu)\right]^{1/2} \qquad (6)$$

with G being the shear modulus, γ_p, the surface energy, and ν, Poisson's ratio. For sample calculation, Petch chose γ_p=10 J/m^2, which, with G=8.2x10^4 MPa and ν=0.28, gives k_c=53.9 N/mm$^{3/2}$. The reduction in k_c, for example, from the 107 N/mm$^{3/2}$ value estimated on a grain size basis by Sandstrom and Bergstrom, becomes increasingly important at small grain sizes.

Bowen and Knott (15) have reported values of the microscopic cleavage fracture stresses determined for a variety of steels, spanning pearlitic, bainitic, and martensitic microstructures, in relation to the width or thickness of the coarsest carbides contained in the materials. Figure 4 shows their results in comparison with several hypothetical cases of different γ_p and ℓ values employed in Equations (5) and (6), plus the condition employed by Petch at the ductile-brittle transition that

$$\sigma_c' \leq \left[\pi k_c^2/(1 + 1/\sqrt{2})k_y\right] \ell^{-1/2} \qquad (7)$$

The Figure shows the transition in behavior between carbide thickness and grain size control of σ_c' for different values of γ_p. For γ_p=10 J/m^2, carbide thickness control occurs for t≥0.4μm when ℓ=10μm and for t≥0.1μm when ℓ=4μm. For γ_p=40 J/m^2, carbide thickness control occurs for t≥0.5μm when ℓ=50μm. The trends which are obtained from these estimates seem reasonable.

The influence of carbide plate thickness on increasing T_c was described by Petch on the basis of Equation (2) but employing an even less complicated constitutive relation for σ_{Th} than is given in Equation (3). Figure 5 shows the result of extending these calculations to finer grain sizes as apply for controlled-rolled steels. Also, the influence of the athermal friction stress, σ_G, on raising T_c is demonstrated. Clearly, the earliest carbide thickness influence on lowering σ_c to σ_c' has the effect of reducing the rate of decrease of T_c with grain size refinement. This is the effect suggested to be involved at σ_y=300 MPa in Figure 3.

Sandstrom and Bergstrom (12) also have reported measurements of maximum carbide plate thickness in their complete study of temperature, strain rate, grain size, and plastic constraint influences on the Charpy V-notch transition properties of C-Mn mild steel. With values of σ_G=130 MPa, k_y=14.9 N/mm$^{3/2}$, and other parameters as given previously, Equation (4) was applied first to computing T_c values. The computed results are given in Table 3 under the heading $T_c(\sigma_c)$, in comparison with the experimentally estimated nil ductility temperatures which were reported. Reasonable agreement is indicated.

The full Charpy curves were reported by Sandstrom and Bergstrom so that a further comparison of transition temperatures can be made. The lowest T_c value in Table 3 is of concern because of the general observation that transition temperatures are increasingly abrupt and well-defined at lower temperatures for finer grain size materials. An explanation of the effect was given by Armstrong (9) on the basis of the steeper increase in yield stress which is observed at lower temperatures. The Charpy curve for the 10 μm grain size material appeared to deviate from this trend in that the change in Charpy energy with temperature was more gradual than that for the 20 μm grain size material. Petch (14) proposed that carbide-initiated cleavage could produce this type of behavior. So, consideration

was given to reducing σ_c to σ_c' in accordance with Equation (5) in order to determine whether improved agreement could be obtained for the transition temperature of the low temperature 10 μm grain size result. With k_c=43 N/mm$^{3/2}$ for γ_p=6.4 J/m^2, the second set of values of $T_c(\sigma_c')$ in Table 3 were obtained. The computed $T_c(\sigma_c')$ values are in accordance with the results shown in Figure 5 of carbide-affected cleavage transition temperatures being raised over the grain size determined ones.

An interesting consequence of the computations given for $T_c(\sigma_c)$ and $T_c(\sigma_c')$ in Table 3 is that the upward shift in transition temperature produced by grain boundary carbide is increasingly larger as the ratio of grain diameter to carbide plate thickness is smaller. The ratio decreases with decrease in grain size in Table 3 from 32.5 to 12.5 to give transition temperature shifts increasing from 14°C to 25°C. This consideration builds on the important result shown in Figure 4, from Bowen and Knott (15), that continued improvement of strength and toughness

Table 3. Comparison of measured (12) and computed grain diameter and carbide thickness influences on ductile-brittle transition temperatures.

Material	B_o, MPa	β_o, °K^{-1}	β_1, °K^{-1}
mild steel	1170	0.0066	0.00034
C-Mn steel	1000	0.0075	0.00040
Armco iron	1033	0.0070	0.00042

properties by grain size refinement requires for grain boundary carbide prone low carbon steels that special attention be given to keeping the carbide thicknesses proportionately much smaller. The requirement becomes especially difficult for ultrafine grain microalloyed steels because of the small carbide dimension which are involved.

SUMMARY

The separate strengthening effects achieved by controlled-rolling over the widest range of finishing temperatures to produce, first, a reduced ferrite grain size and, then, an increased athermal friction stress give opposite influences of lowering and raising the Charpy FATT, respectively. This result is in agreement with predictions from the dislocation mechanics based Hall-Petch stress-grain size equations. An important part of the improved FATT properties achieved for a C-Mn-Mo-Nb steel is attributed to the enhanced grain size reduction and lowered athermal friction stress obtained by finish rolling austenite in a two-phase field containing a relatively strong, high temperature Mo solution strengthened, ferrite constituent. Grain boundary carbide plates give an increasingly raised FATT at ultrafine grain sizes through lowering the pile-up stress intensity needed for cleavage fracturing, particularly, at small ratios of grain diameter and carbide plate thickness where the individual dimensions are experimentally difficult to measure.

REFERENCES

1. G. R. Speich and D. S. Dabkowski, The Hot Deformation of Austenite, ed. J. B. Ballance (New York, NY: American Institute of Mining, Metallurgical and Petroleum Engineers, 1979), 557.
2. E. O. Hall, "The Deformation and Ageing of Mild Steel: III. Discussion of Results", Proc. Phys. Soc. London., B64 (1951) 747.
3. N. J. Petch, "The Cleavage Strength of Polycrystals",J. Iron Steel Inst., 174 (1953) 25.
4. R. W. Armstrong, Yield, Flow and Fracture of Polycrystals, ed. T. N. Baker (London, UK: Applied Science Publishers, 1983), 1.
5. W. B. Morrison, "The Effect of Grain Size on the Stress-Strain Relationship in Low-Carbon Steel", Trans ASM, 59 (1966) 824.
6. J. Heslop and N. J. Petch, "The Ductile-Brittle Transition in the Fracture of α-Iron: II", Phil. Mag., 3 (1958) 1128.
7. R. W. Armstrong, "On Determining the Ductile-Brittle Transition Temperature", Phil. Mag., 9 (1964) 1063.
8. R. W. Armstrong, Fracture 1969 (London, UK: Chapman and Hall Ltd, 1969), 314.
9. R. W. Armstrong, "The Influence of Polycrystal Grain Size on Several Mechanical Properties of Materials", Metall. Trans., 1 (1970) 1169.
10. R. W. Armstrong, "Relation between the Petch Friction Stress and the Thermal Activation Rate Equation", Acta Metall., 25 (1967) 667.
11. D. A. Curry, "Predicting the Temperature and Strain Rate Dependences of the Cleavage Fracture Toughness of Ferritic Steels", Mater. Sci. Eng., 43 (1980) 135.
12. R. Sandstrom and Y. Bergstrom, "Relationship between Charpy V Transition Temperature in Mild Steel and Various Material Parameters", Metal Sci., 18 (1984) 177.

13. F. J. Zerilli and R. W. Armstrong,"Dislocation-Mechanics-Based Constitutive Relations for Material Dynamics Calculations", J. Appl. Phys., 61 (1987) 1816.

14. N. J. Petch,"The Influence of Grain Boundary Carbide and Grain Size on the Cleavage Strength and Impact Transition Temperature of Steel", Acta Metall., 34 (1986) 1387.

15. P. Bowen and J. F. Knott, Strength of Metals and Alloys, ICSMA-7-CIRMA, eds. J.-P. Bailon, J. I. Dickson, J. J. Jonas, and M. G. Akben (New York, NY: Pergamon Press, 1985), Vol. 2, 1111.

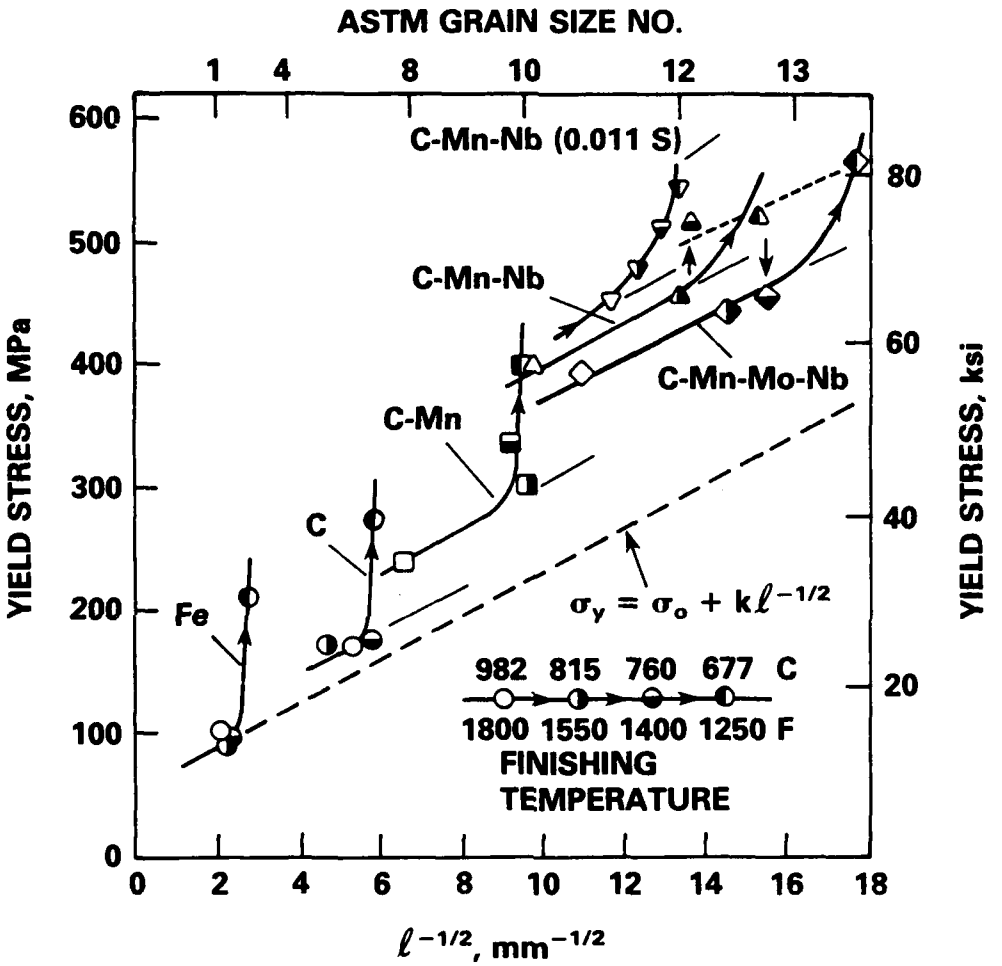

Fig. 1. Yield stress, σ_y, versus reciprocal square root of grain diameter, $\ell^{-\frac{1}{2}}$, for different controlled-rolled steels.

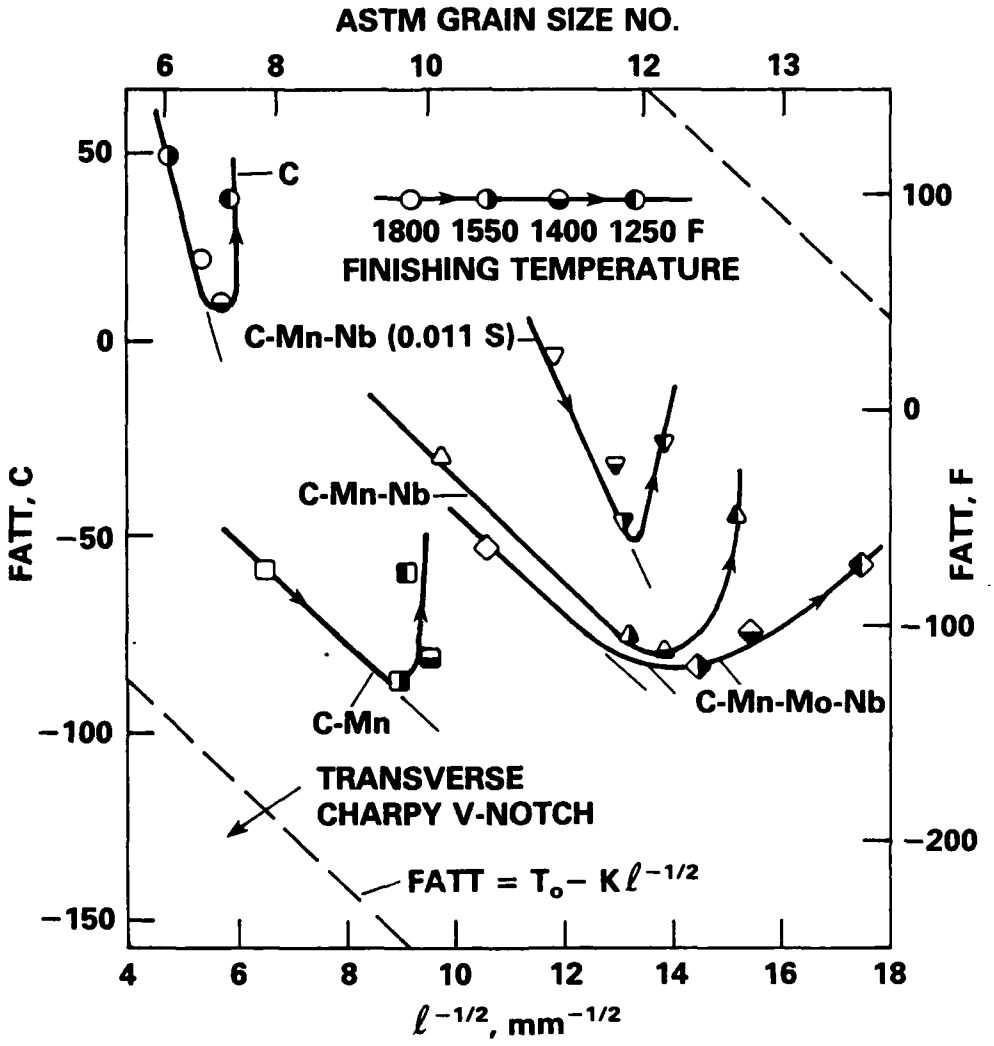

Fig. 2. Fracture appearance transition temperature (FATT) versus $\ell^{-\frac{1}{2}}$ for different controlled-rolled steels.

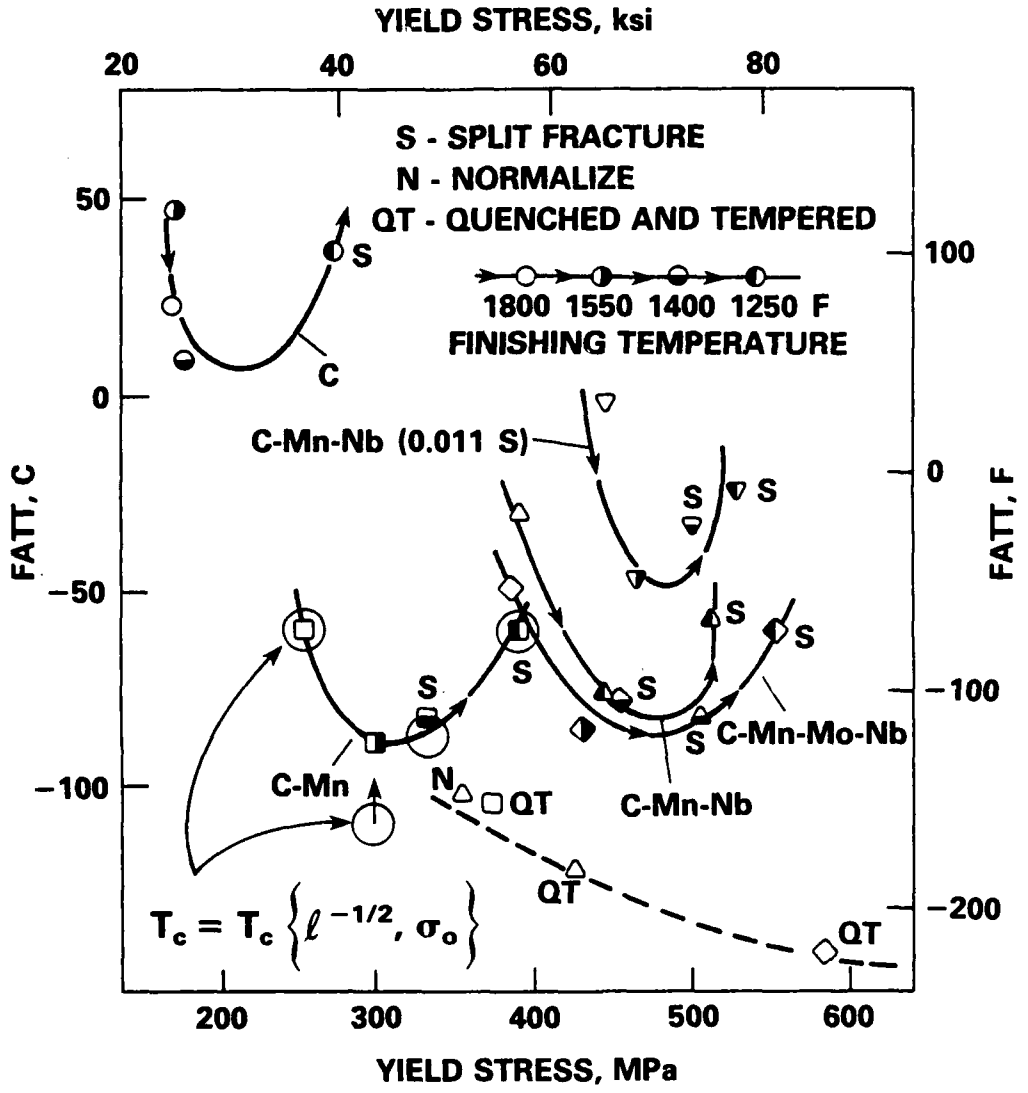

Fig. 3. FATT versus σ_y for different controlled-rolled steels, with computed transition temperatures, T_c, for C-Mn steel.

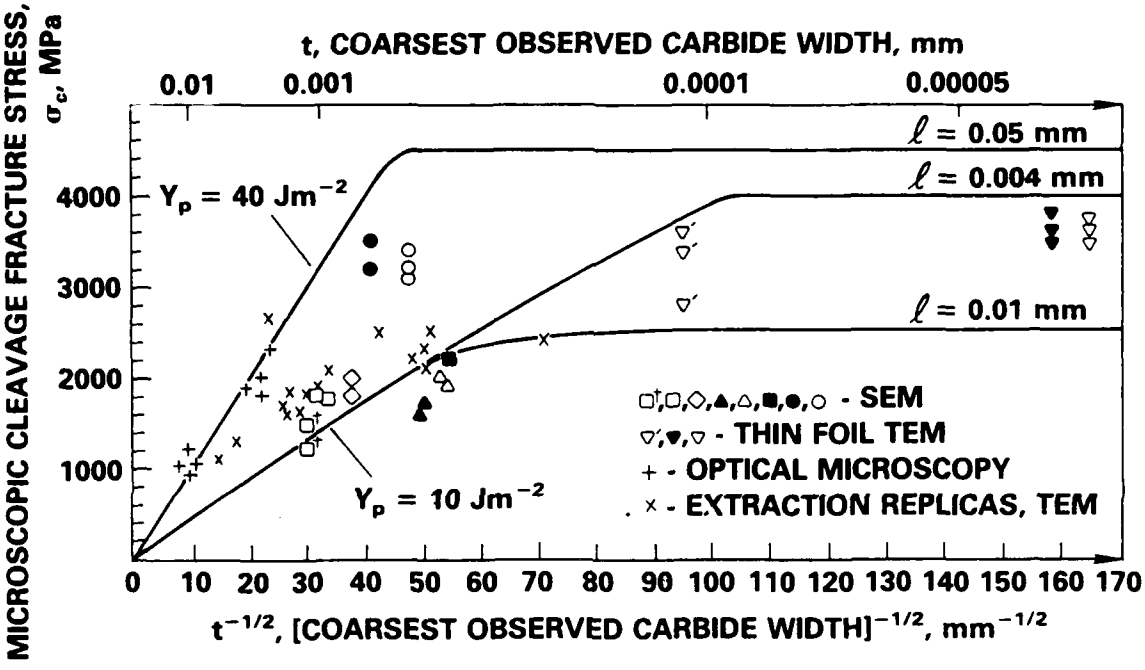

Fig. 4. Microscopic cleavage fracture stress dependence on reciprocal square root of carbide plate thickness or width, $t^{-\frac{1}{2}}$, for a variety of steel microstructures, in comparison with the computed σ_c' dependence on $t^{-\frac{1}{2}}$ for different grain diameters.

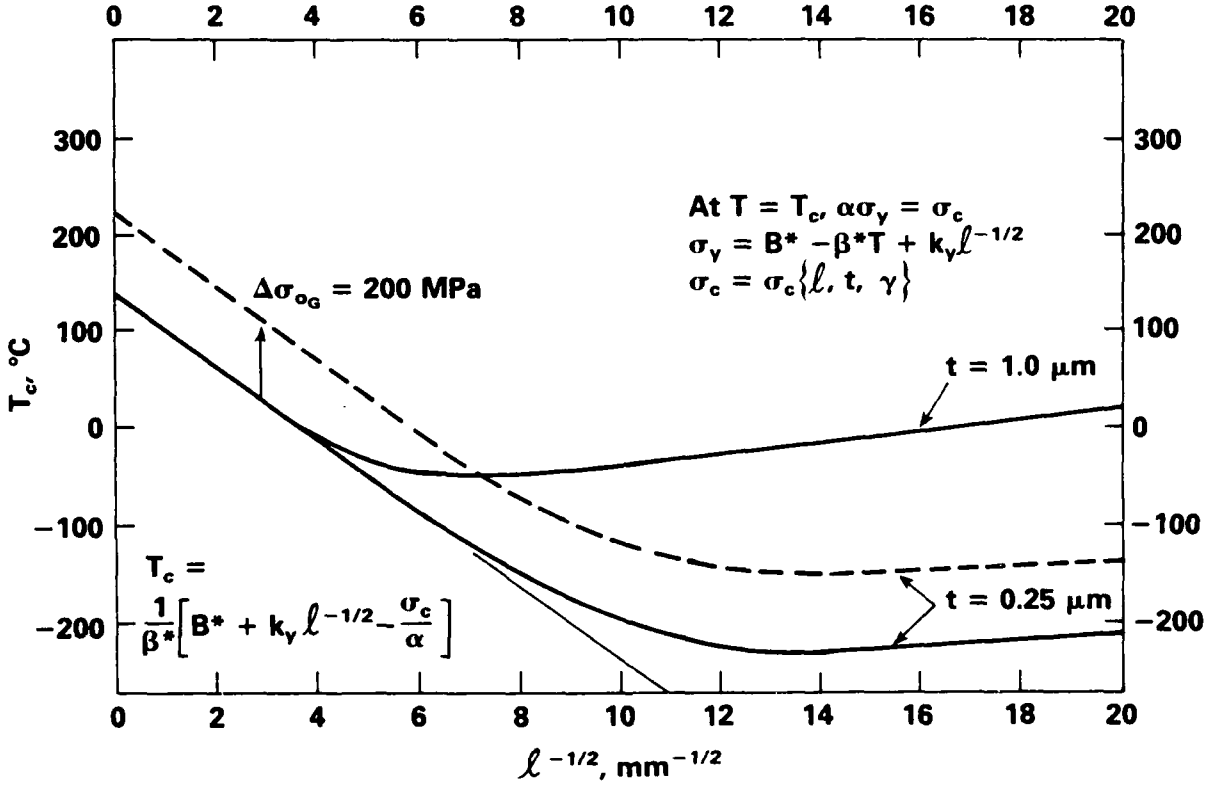

Fig. 5. Computed T_c dependence on $\ell^{-\frac{1}{2}}$ for different carbide thicknesses, t, and friction stresses, σ_G.

INITIAL DISTRIBUTION

Copies		CENTER DISTRIBUTION Copies	Code
1	DDRE/Lib	1	012.3
		2	012.5
1	CNO/OP 098T	1	17
		1	172
2	OCNR	2	172.4
	1 432S	1	172.5
	1 Library	1	173
		1	173.3
1	NAVPGSCOL	1	174
		1	174.3
1	USNROTCU	1	174.4
	NAVADMINU MIT	1	28
		1	2801
2	NRL	2	2803
	1 Code 6380	1	2809
	1 Code 6384	5	281
		1	2812
20	NAVSEA	1	2812 (TMS)
	1 SEA C5M	5	2814
	1 SEA 05MB	25	2814 (LRL)
	2 SEA 05M2	1	2814 (MEN)
	1 SEA 05R	1	2814 (MGV)
	1 SEA 05R25	1	2815
	1 SEA 05R26	1	522.2
	2 SEA 08S	2	5231
	1 SEA 55Y		
	1 SEA 55Y1		
	1 SEA 55Y12		
	1 SEA 55Y2		
	1 SEA 55Y21		
	1 SEA 55Y22		
	1 SEA 55Y23		
	1 SEA 55Y3		
	1 SEA 55Y31		
	2 SEA 99612		
12	DTIC		

END

DATE

FILMED

DTIC

10-88